

Direct Visualization of Transient Thermal Response of a DNA Origami

Jie Song,^{†,‡} Jean-Michel Arbona,[§] Zhao Zhang,^{†,||} Lei Liu,[†] Erqing Xie,[‡] Juan Elezgaray,[§] Jean-Pierre Aime,[§] Kurt Vesterager Gothelf,^{†,||} Flemming Besenbacher,^{*,†} and Mingdong Dong^{*,†}

[†]Centre for DNA Nanotechnology (CDNA) at the Interdisciplinary Nanoscience Center (iNANO), Aarhus University, DK-8000 Aarhus C, Denmark

[‡]School of Physical Science and Technology, Lanzhou University, Lanzhou 730000, People's Republic of China

[§]CBMN, UMR 5248, CNRS, 2 rue R. Escarpit, 33600 Pessac, France

^{||}Department of Chemistry, Aarhus University, DK-8000 Aarhus C, Denmark

S Supporting Information

ABSTRACT: The DNA origami approach enables the construction of complex objects from DNA strands. A fundamental understanding of the kinetics and thermodynamics of DNA origami assembly is extremely important for building large DNA structures with multifunctionality. Here both experimental and theoretical studies of DNA origami melting were carried out in order to reveal the reversible association/disassociation process. Furthermore, by careful control of the temperature cycling via in situ thermally controlled atomic force microscopy, the self-assembly process of a rectangular DNA origami tile was directly visualized, unveiling key mechanisms underlying their structural and thermodynamic features.

Structural DNA nanotechnology, which makes use of DNA as a building block of self-assembly for the construction of arbitrary shapes, has proven to be an efficient route for building new functional objects with increasing complexity.¹ The recent development of the DNA origami approach,² in which a long “scaffold” strand derived from a viral genome (M13mp18) can be folded with hundreds of short ssDNA oligos called “staples”, allows the arrangement of thousands of nucleotides with subnanometer precision at specified locations in space to yield geometrically defined two-dimensional (2D)² and three-dimensional (3D) nanoarchitectures.^{3–7} Taking advantage of the sequence specificity and the resulting spatial addressability, various elegant single-molecule studies have employed these DNA nanoarchitectures to investigate chemical reactions,⁸ organization of heteroelements,^{9,10} complex molecular robots,^{11–13} and so on.

However, exactly as pointed by Shih, Yan, and co-workers,¹⁴ long-term progress toward the construction of large DNA structures or complex functional DNA materials will require a further understanding of both the theoretical and the practical possibilities of the self-assembly process during a thermal annealing process according to the energetic rule. DNA melting studies are considered as an extremely valuable tool for obtaining a better understanding of the essential factors for the assembly of increasingly complex DNA nanostructures.¹⁵ Especially, much effort is required in combining modeling and experimental studies to investigate the sequence of association and the correlation governing the pairing of staple

strands to the scaffold.^{16,17} Niemeyer and co-workers¹⁸ used temperature-dependent Förster resonance energy transfer (FRET) spectroscopy for real-time monitoring of the self-assembly of DNA cross-tiles into nanoarrays. Dietz and co-workers¹⁹ measured the melting profiles of multihelix-bundle origami by collecting the fluorescence intensity of a reporter dye. A melting transition between 55 and 65 °C was observed for typical DNA origami structures, and Sugiyama and co-workers²⁰ found that this could be increased by at least 80 °C after photo-cross-linking with 8-methoxypsoralen. Despite those innovative explorations, the folding process of DNA origami, such as the order of association of staple strands to form the scaffold, still remains poorly understood, and thus, in situ single-molecule imaging techniques should be implemented to obtain direct evidence and visualization.

In this work, we demonstrated how thermally controlled atomic force microscopy (AFM) with carefully chosen temperature cyclings can be used as a powerful tool to reveal the temperature-dependent dynamic characteristics of the assembly of DNA origami structures. Figure 1a shows an illustration of the thermally controlled AFM experiment. A piezoscanner with an additional heating element offered a suitable platform for the thermally responsive experiment as the temperature was increased from room temperature (RT) up to 80 °C. A rectangular DNA origami tile² (measured ~100 nm × 70 nm; Figure 1b) was used as a model test object in our experiments. The annealing method and other experimental details are given in the Supporting Information (SI). When samples were deposited on the heating substrate, DNA origami tiles were immobilized on the surface, and the same area (dashed box in Figure 1c) was scanned by AFM as the temperature was gradually increased from 50 to 75 °C in steps of 5 °C (Figure 1d). No changes were observed below 50 °C (data not shown). The heating rate was controlled at 1 °C/min. The origami chain formed by base pairing began to disassemble after reaching 55 °C, while significant local defects emerged at 60 °C and were enlarged at 65 °C. Further increasing the temperature induced melting of the whole DNA origami. When the temperature reached 75 °C, most of the DNA origami fell in tatters and eventually disappeared with 10 min of sustained

Received: February 23, 2012

Published: May 30, 2012

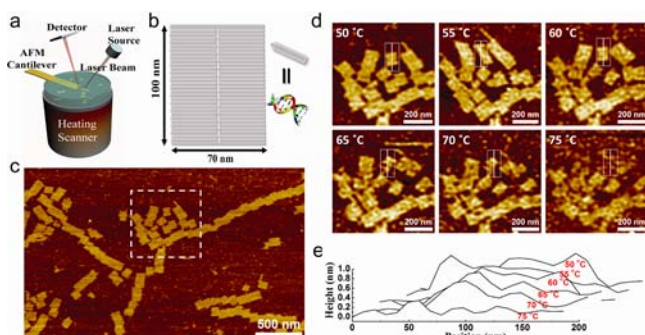


Figure 1. (a) Illustration of thermally controlled AFM in liquid. (b) Model of the “tall rectangle” DNA. (c) Typical AFM image of the prior-annealed “tall rectangle” DNA at a scanning temperature of 50 °C. (d) In situ AFM images with careful stepwise control of the scanning temperature from 50 to 75 °C. (e) Height profiles of a single origami as scanned along the line sketched in (d).

scanning. To obtain quantitative changes during the melting process, eight profiles of a chosen single origami (corresponding to the white line in Figure 1d) were monitored during the heating process (Figure 1e). An obvious decrease in height with increasing temperature was clearly observed, and by 75 °C the height profile was almost down to the baseline. The decreasing in height of the DNA origami in the AFM images is due to disassembly of the oligo from the scaffold. Furthermore, it was observed that the vast majority of the local defects, especially at 65 °C, were distributed along the edges of the rectangles.

On the basis of the above observations, it was necessary to execute more quantitative analysis of the height changes at different temperatures. The curve shown in Figure 2a was calculated statistically from a height histogram over multiple origami (Figure S1 in the SI). It indicates that the melting transition of the DNA origami on the mica surface began at ~55 °C, which seems well-consistent with the fluorescence

microscopy results of Dietz and co-workers,¹⁹ although it is worth noticing that the test object we employed here was a 2D planar origami rather than a 3D origami as in their experiment. More importantly, our melting experiments were performed on a solid–liquid interface instead of a bulk environment, which might account for the higher thermal tolerance here. The height deformation slope ranged over 20 °C (from 55 to 75 °C), which distinctly implied that various staples dissociated from the long scaffold should have different intrinsic stabilities.

To explain the above phenomena, a theoretical model was applied to simulate the melting process of origami in solution. This model takes into account the interactions between staples and the resulting cooperativity. The hybridization of any staple to the structure locally decreases the entropy of the scaffold, facilitating the binding of neighboring staples.^{16,17} On the basis of the fact that double-stranded DNA has a lower absorbance at 260 nm than single-stranded DNA,¹⁵ theoretical UV absorption data were simulated (Figure 2b). The model predicted that the melting transition should start at ~55 °C and be complete at ~70 °C, which is ~10 °C lower than the experimental results. Meanwhile, we noted that though the melting process spanned 20 °C (as shown above), the average melting temperature (~60 °C) was comparable with those calculated for the individual staple oligonucleotide sequences used in the design.²¹ Overall, these results show a stabilization relative to the model of the free origami, which could be attributed to a surface anchoring effect and to a reduction of the scaffold entropy.²² The AFM manipulation during scanning could also have an influence on the DNA origami. Furthermore, Figure 2c shows a map of the melting temperatures of the staples on the origami (the melting temperature of an individual staple corresponds to a staple hybridization probability of 0.5). Considering the homogeneity of the mica surface, the effect of origami–surface interactions was ignored in the modeling. It can be observed that top and bottom staples have higher melting temperatures. This could be due to areas rich in G and C bases, which result in increased

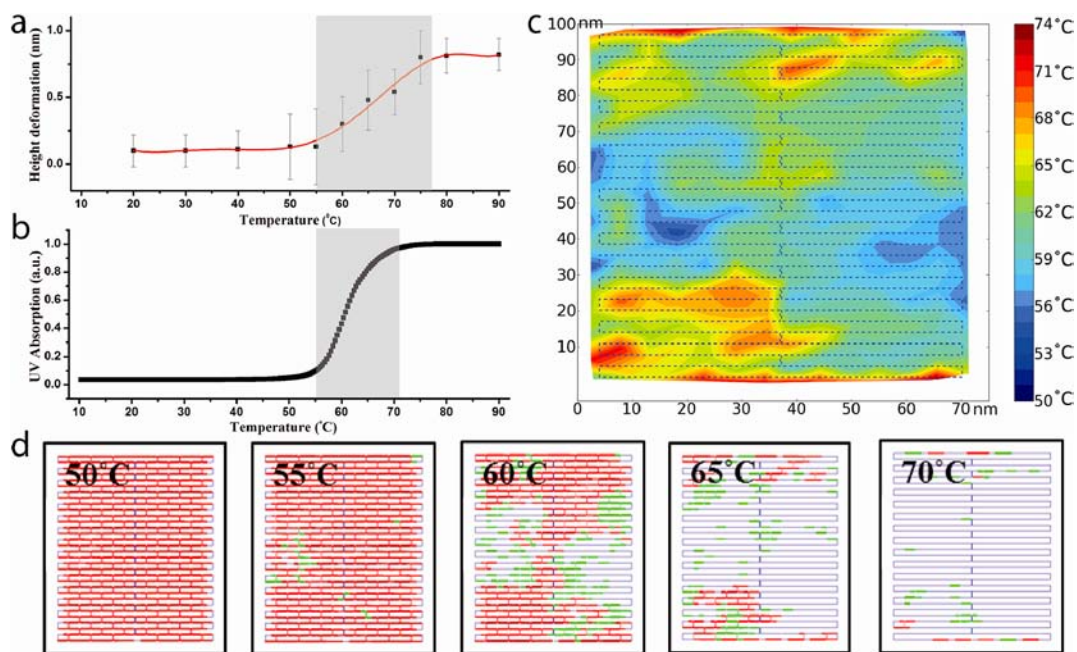


Figure 2. (a) Height deformation analysis of the “tall rectangle” DNA. (b) Theoretical UV absorption data. (c) Melting temperature map for the individual rectangle DNA origami. (d) Simulation images at different temperature stages. The colors represent the ratio of folded staple (r): red, $r > 0.5$; green, $0.5 > r > 0.05$.

melting temperatures.^{23,24} (For more information about the G–C fraction map and the sequence details, see Figures S4–S6). It is also interesting that the staples beside the middle bridged seam have lower melting temperatures than the staples inside the seam (Figure S3).

On the other hand, simulations of the DNA origami at different temperatures (Figure 2d; for more results, see the video in the SI) clearly demonstrated that the staples dissociated from the scaffold in a specific order. Particularly, by 60 °C, the staples beside the bridged seam were almost totally unfolded as a result of the enriched G–C content. Besides, as shown in Figure 1d, most of the hole defects first appeared along the edges of the rectangles. To some extent, this indicated that these staples beside the bridged seam presented lower melting temperatures, which induced the hole defects along the edges.

Inspired by our success in revealing the structural and thermodynamic features of the dissociation process, we attempted to study the possible reassociation process. Initially a sample was heated continuously to 75 °C, where all of the origami were completely disrupted (Figure 3a, middle). The

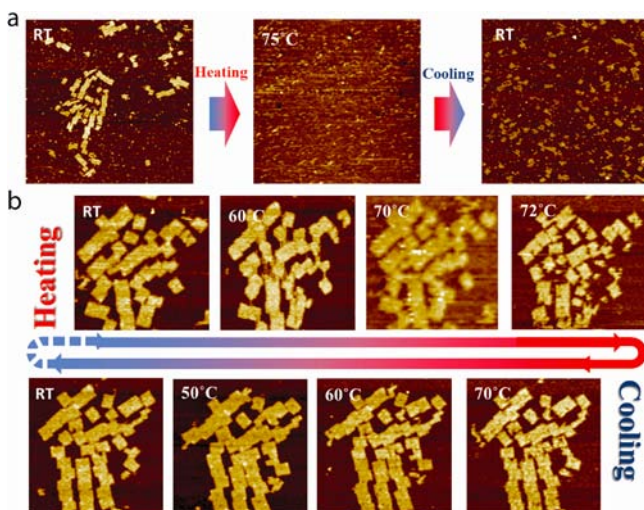


Figure 3. (a) In situ AFM images under continuous heating from RT to 75 °C at a rate of 2 °C/min followed by natural cooling to RT in the presence of excess staples (100 nM). The scanning area was 3 μm \times 3 μm . (b) Cycling process with heating to 72 °C at a rate of 2 °C/min followed by cooling to RT at a rate of 1 °C/min. The scanning area was 0.7 μm \times 0.7 μm .

sample was then rapidly cooled back to RT in less than 20 min while being scanned. Some of the staples recovered to the same extent as in the bulk annealing, where normally an excess of staples must be added.² Not surprisingly, most of them failed to engage in the origami assembly, leaving fragmentary DNA tiles only, as a result of the challenge of recovering from the relatively rapid annealing in this experiment.

Further investigation was performed by carefully controlling the temperature and monitoring the process at intervals of 10 °C. The samples were heated at a rate of 2 °C/min from RT as before, but this time up to only 72 °C instead of 75 °C, where a completely disrupted structure had been obtained. The partially disrupted structure at 72 °C (Figure 3b, top-right), with some of the tiles melted into different pieces and others having several hole defects near the edges, could be used as a target to allow a discernible contour of origami structures. The chamber

was then carefully cooled from 72 to 50 °C at a rate of 1 °C/min. For the reassembly process, a large excess of the staples (100 nM) was added to the AFM cell. It can be observed that just at the beginning of the cooling process (e.g., at 70 °C), most of the fragments had been reconstructed into the customary rectangular shape again, although some hole defects were still present (Figure 3b, bottom-right). Interestingly, at the same time, the stacking force also came into play, quickly resulting in local rearrangement of the origami on the surface. Further cooling to 60 °C (Figure 3b, bottom-right-middle) mostly eliminated the hole defects, while at 50 °C, almost all of the prominent defects had been repaired. Then another cooling process lasted less than 30 min until the temperature reached RT, at which point regeneration of DNA origami rectangles was accomplished (Figure 3b, bottom-left). In comparison with the overheated process (75 °C, Figure 3a), most of the origami were recovered locally without changing position. Therefore, it is easy to see that the DNA nanostructures can repeatedly go through such heating–cooling multicycles in a molecular assembly/disassembly process. Microscopy has been used for investigating the thermal stability of DNA structures or even origami,^{15,20,25} but only independent samples at different temperature stages have been studied. To our knowledge, this is the first time that the origami assembly process has been tracked in situ, which holds great potential for exploring the thermodynamic properties. Without doubt, it will contribute to improving both the annealing procedure and the original staple design and understanding the mechanisms underlying surface-mediated DNA self-assembly^{26,27} and programming of geometric arrangements of origami.²⁸

In conclusion, a powerful platform based on thermally controlled AFM has been developed for in situ visualization of the reversible molecular self-assembly processes of DNA origami. The interplay between theoretical predictions and experimental measurements showed that the local staples beside the bridged seam contribute significantly to the initial disassembly. Their contribution can be tuned via the local position and the sequence, even on surface supports with a relatively low mobility. In situ monitoring of the transient thermal response combined with high-resolution imaging allows accurate study of versatile DNA and DNA complexes self-assembled on surfaces without labeling, opening new possibilities for the design and construction of DNA-based devices locally down to a certain region within the origami while retaining the initial structural nature on the surface. In general, the direct visualization via thermally controlled AFM can also be applied to other biological systems to understand the thermal effects in terms of structures and functions.

■ ASSOCIATED CONTENT

📄 Supporting Information

Materials and experimental methods, sequence of the rectangle DNA origami, additional AFM images and height cartograms, discussion of the G–C content, and a video file (AVI). This material is available free of charge via the Internet at <http://pubs.acs.org>.

■ AUTHOR INFORMATION

✉ Corresponding Author

fbe@inano.au.dk; dong@inano.au.dk

Notes

The authors declare no competing financial interest.

■ ACKNOWLEDGMENTS

This work was supported by grants from the Danish National Research Foundation to the CDNA Centre and the Danish Research Agency through support for the iNANO Center. M.D. acknowledges a STENO Grant from the Danish Research Council and the VKR Young Investigator Program in Denmark. J.S. acknowledges a Ph.D. Scholarship from the China Scholarship Council of the Ministry of Education of China. This work also benefited from the support of COST TD1003 Action. We sincerely thank Professor Hendrik Dietz (Technische Universität München, Germany) for fruitful discussions and suggestions.

■ REFERENCES

- (1) Seeman, N. C. *Annu. Rev. Biochem.* **2010**, *79*, 65–87.
- (2) Rothmund, P. W. K. *Nature* **2006**, *440*, 297–302.
- (3) Douglas, S. M.; Dietz, H.; Liedl, T.; Hogberg, B.; Graf, F.; Shih, W. M. *Nature* **2009**, *459*, 414–418.
- (4) Andersen, E. S.; Dong, M.; Nielsen, M. M.; Jahn, K.; Subramani, R.; Mamdouh, W.; Golas, M. M.; Sander, B.; Stark, H.; Oliveira, C. L. P.; Pedersen, J. S.; Birkedal, V.; Besenbacher, F.; Gothelf, K. V.; Kjems, J. *Nature* **2009**, *459*, 73–76.
- (5) Dietz, H.; Douglas, S. M.; Shih, W. M. *Science* **2009**, *325*, 725–730.
- (6) Han, D.; Pal, S.; Liu, Y.; Yan, H. *Nat. Nanotechnol.* **2010**, *5*, 712–717.
- (7) Han, D.; Pal, S.; Nangreave, J.; Deng, Z.; Liu, Y.; Yan, H. *Science* **2011**, *332*, 342–346.
- (8) Voigt, N. V.; Topping, T.; Rotaru, A.; Jacobsen, M. F.; Ravnsbaek, J. B.; Subramani, R.; Mamdouh, W.; Kjems, J.; Mokhir, A.; Besenbacher, F.; Gothelf, K. V. *Nat. Nanotechnol.* **2010**, *5*, 200–203.
- (9) Ke, Y.; Lindsay, S.; Chang, Y.; Liu, Y.; Yan, H. *Science* **2008**, *319*, 180–183.
- (10) Subramani, R.; Juul, S.; Rotaru, A.; Andersen, F. F.; Gothelf, K. V.; Mamdouh, W.; Besenbacher, F.; Dong, M.; Knudsen, B. R. *ACS Nano* **2010**, *4*, 5969–5977.
- (11) Gu, H.; Chao, J.; Xiao, S.; Seeman, N. C. *Nat. Nanotechnol.* **2009**, *4*, 245–248.
- (12) Lund, K.; Manzo, A. J.; Dabby, N.; Michelotti, N.; Johnson-Buck, A.; Nangreave, J.; Taylor, S.; Pei, R.; Stojanovic, M. N.; Walter, N. G.; Winfree, E.; Yan, H. *Nature* **2010**, *465*, 206–210.
- (13) Wickham, S. F. J.; Endo, M.; Katsuda, Y.; Hidaka, K.; Bath, J.; Sugiyama, H.; Turberfield, A. J. *Nat. Nanotechnol.* **2011**, *6*, 166–169.
- (14) Pinheiro, A. V.; Han, D.; Shih, W. M.; Yan, H. *Nat. Nanotechnol.* **2011**, *6*, 763–772.
- (15) Sobey, T. L.; Renner, S.; Simmel, F. C. *J. Phys.: Condens. Matter* **2009**, *21*, No. 034112.
- (16) Arbona, J. M.; Aimé, J.-P.; Elezgaray, J. *J. Chem. Phys.* **2012**, *136*, No. 065102.
- (17) The model solves a series of coupled kinetic reactions that describe the binding of each staple to the origami. To make this system solvable, we made several assumptions. The fundamental assumption was a locality assumption, which states that the binding depends only on how many nearby staples are already bound to the origami. Besides the usual dependence with respect to sequence (nearest-neighbor model, Santa Lucia model, etc.), we added a topological term to the free energy of binding. The basic idea here is that the binding of other staples reduces the entropy of the scaffold, resulting in a cooperative effect. The parametrization of these topological terms was based on UV measurements made on small DNA constructs with only three single-stranded DNA with lengths of 32, 32, and 64 nucleotides.
- (18) Sacca, B.; Meyer, R.; Niemeyer, C. M. *Nat. Protoc.* **2009**, *4*, 271–285.
- (19) Castro, C. E.; Kilchherr, F.; Kim, D.; Shiao, E. L.; Wauer, T.; Wortmann, P.; Bathe, M.; Dietz, H. *Nat. Methods* **2011**, *8*, 221–229.
- (20) Rajendran, A.; Endo, M.; Katsuda, Y.; Hidaka, K.; Sugiyama, H. *J. Am. Chem. Soc.* **2011**, *133*, 14488–14491.
- (21) Zuker, M. *Nucleic Acids Res.* **2003**, *31*, 3406–3415.
- (22) Leunissen, M. E.; Dreyfus, R.; Sha, R.; Seeman, N. C.; Chaikin, P. M. *J. Am. Chem. Soc.* **2010**, *132*, 1903–1913.
- (23) SantaLucia, J., Jr.; Hicks, D. *Annu. Rev. Biophys. Biomol. Struct.* **2004**, *33*, 415–440.
- (24) Nangreave, J.; Yan, H.; Liu, Y. *Biophys. J.* **2009**, *97*, 563–571.
- (25) O'Neill, P.; Rothmund, P. W. K.; Kumar, A.; Fyngenson, D. K. *Nano Lett.* **2006**, *6*, 1379–1383.
- (26) Sun, X.; Hyeon, K. S.; Zhang, C.; Ribbe, A. E.; Mao, C. *J. Am. Chem. Soc.* **2009**, *131*, 13248–13249.
- (27) Hamada, S.; Murata, S. *Angew. Chem., Int. Ed.* **2009**, *48*, 6820–6823.
- (28) Woo, S.; Rothmund, P. W. K. *Nat. Chem.* **2011**, *3*, 620–627.